

# A Long Fluorescence Lifetime Probe for Labeling of Gram-Negative Bacteria

Assel Baibek, Zuzanna Konieczna, Muhammed Üçüncü, Zainab S. Alghamdi, Richa Sharma, Mathew H. Horrocks, and Mark Bradley\*

Cite This: *Chem. Biomed. Imaging* 2025, 3, 45–50

Read Online

ACCESS |

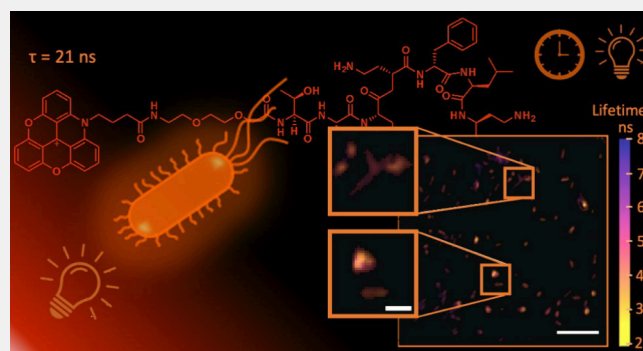
Metrics & More

Article Recommendations

Supporting Information

**ABSTRACT:** Bacterial resistance, primarily stemming from misdiagnosis, misuse, and overuse of antibacterial medications in humans and animals, is a pressing issue. To address this, we focused on developing a fluorescent probe for the detection of bacteria, with a unique feature—an exceptionally long fluorescence lifetime, to overcome autofluorescence limitations in biological samples. The polymyxin-based probe (ADOTA-PMX) selectively targets Gram-negative bacteria and used the red-emitting fluorophore azadioxatriangulenium (with a reported fluorescence lifetime of 19.5 ns). Evaluation of ADOTA-PMX's bacterial labeling efficacy revealed strong specificity for Gram-negative bacteria, and full spectral fluorescence lifetime imaging microscopy demonstrated the potential of ADOTA-PMX for bacterial imaging applications. The probe exhibited a lifetime of 4.5 ns when bound to bacteria, possibly indicating interactions with the bacterial outer membrane. Furthermore, the fluorescence lifetime measurements of ADOTA-PMX labeled bacteria could be performed using a benchtop fluorimeter without the need of sophisticated microscopes. This study represents the first targeted probe for fluorescence lifetime imaging, offering sensitivity for detecting Gram-negative bacteria and enabling multiplexing via fluorescence lifetime imaging.

**KEYWORDS:** fluorescence lifetime imaging, bacteria targeting, bacterial detection, optical imaging, fluorescent probe, polymyxin probe



The primary causes of bacterial resistance are the misuse, and excessive administration, of antibiotics in humans and animals.<sup>1,2</sup> Developing new diagnostic techniques that could quickly and accurately identify infections caused by specific microorganisms would be highly beneficial in focusing on antibacterial use. Targeted imaging of the bacteria using various probes has been reviewed and includes antibody-fluorophore conjugates, aptamer-based probes, metabolically incorporable probes, fluorescent proteins, and a variety of small molecule-based probes. These diverse approaches give a broad toolkit for imaging bacterial infections in different models.<sup>3,4</sup> This includes fluorescent probes that label bacteria, or are activated by specific bacterial enzymatic with many created by the attachment of fluorophores to specific antimicrobial agents.<sup>5</sup> These include  $\beta$ -lactam based probes with penicillins labeled with BODIPY-based fluorophores,<sup>6</sup> cephalosporins labeled with a Förster resonance energy transfer (FRET) pair<sup>7,8</sup> designed to switch-on in the presence of  $\beta$ -lactam cleaving proteins by turnover, or covalent labeling of penicillin-binding proteins. Such probes can be used to assess the resistance profile of bacterial species to  $\beta$ -lactam antibiotics, although the spectrum of resistance profiles against  $\beta$ -lactam-containing antibiotics is huge.

Other classes of bacterial probes based on other antibacterial agents have been widely reported. This includes the antimicrobial peptide ubiquicidin 29–41 (UBI<sub>29–41</sub>), initially applied as a <sup>99m</sup>Tc-labeled peptide for the imaging of infection.<sup>9</sup> A modified variant of this peptide was subsequently synthesized as a fluorogenic tribranched nitrobenzoxadiazole (NBD) labeled ( $\lambda_{\text{ex}} = 488 \text{ nm}$ ) probe that was used to image bacteria.<sup>10,11</sup> Attachment of a near-infrared fluorophore to this peptide has also used to detect *in vivo* bacterial infection in mice models.<sup>12</sup> Dual radioactive/fluorogenic tracers, such as <sup>99m</sup>Tc-UBI<sub>29–41</sub>-Cy5, allowed multimodal *in vivo* imaging of bacteria via single photon emission computerized tomography, SPECT and fluorescence.<sup>13</sup>

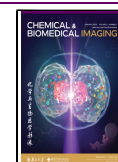
A variety of other probes have been reported for selective labeling of bacteria, such as those based on the glycopeptide Vancomycin that is an inhibitor of peptidoglycan cross-linking.<sup>14</sup> For example, BODIPY-labeled Vancomycin ( $\lambda_{\text{ex}} =$

**Received:** September 18, 2024

**Revised:** November 26, 2024

**Accepted:** November 27, 2024

**Published:** December 5, 2024



488 nm) was used for bacteria quantification in flow cytometry,<sup>15</sup> Vanco-Cy3 ( $\lambda_{\text{ex}} = 555$  nm) was used for labeling the gut microbiotas in mice,<sup>16</sup> and Vanco-800CW ( $\lambda_{\text{ex}} = 745$  nm) was used for real-time *in vivo* imaging of bacteria in a mouse myositis model.<sup>17</sup> Two “no-wash” probes were developed using solvato-fluorogenicity. Thus, Merocy-Van ( $\lambda_{\text{ex}} = 590$  nm) was used for the detection of bacteria in a human lung<sup>18</sup> and an NBD-Vancomycin probe ( $\lambda_{\text{ex}} = 488$  nm) was used for analysis of human eye<sup>19</sup> infections. Another antibiotic linezolid, was applied in the optical imaging of bacteria via conjugation of the fluorophore DMACA ( $\lambda_{\text{ex}} = 350$  nm) or NBD through “click” cycloaddition chemistry.<sup>20</sup>

Despite the wide array of fluorescent probes that have been developed, autofluorescence in biological samples can limit the signal-to-background ratio, making probes poorly visible<sup>21</sup> and restricting their ability to quantify biomarkers. Another property of fluorophores that can be measured is their fluorescence lifetime, which is typically independent of their concentration. Fluorescence lifetime can be used in tandem with fluorescence intensity allowing multiple fluorophores within the same spectral region to be distinguished, thus facilitating multiplexed imaging.<sup>21</sup> Some dyes also display altered fluorescence lifetimes, depending on their local environment, which can be advantageous for cell or organelle-specific probes.<sup>22,23</sup> Traditionally, analysis of fluorescent lifetime has been limited by the speed of detectors and rates of data transfer; however, recently reported CMOS SPAD-based detectors with on-chip “histogram” generation have overcome many of these challenges.<sup>24</sup> Most of the state-of-the-art probes described above use fluorophores with quite commonly observed fluorescent lifetimes (e.g., for Cy3,  $\tau = 0.18$ – $1.8$  ns;<sup>25</sup> for NBD,  $\tau = 0.9$  ns (in water environment);<sup>26</sup> for 800CW,  $\tau = 0.74$  ns).<sup>27</sup> These are hard to extinguish from those of common endogenous fluorophores (e.g., for NAD(P)H protein bound,  $\tau = 2.0$ – $2.3$  ns; for FAD free,  $\tau = 2.91$  ns; for tryptophan,  $\tau = 3.09$  ns).<sup>28</sup>

Herein, we developed a fluorescent probe that was selective for Gram-negative bacteria but with the specific feature of the fluorophore exhibiting an exceptionally long lifetime. To achieve this, polymyxin (PMX) was chosen as the targeting ligand, since it has been widely utilized in the development of probes for both imaging and photodynamic killing of a range of Gram-negative bacteria (e.g., *E. coli* as free-floating planktonic cells and in biofilms) with the use of variety of fluorophores (Cy3, NBD, Merocyanine, Methylene Blue).<sup>29–32</sup> To fulfill the requirement of a long fluorescence lifetime azadioxatriangulenium (ADOTA (2)) was chosen as a signaling moiety, due to its reported lifetime of 19.5 ns (in phosphate buffered saline (PBS)).<sup>33</sup>

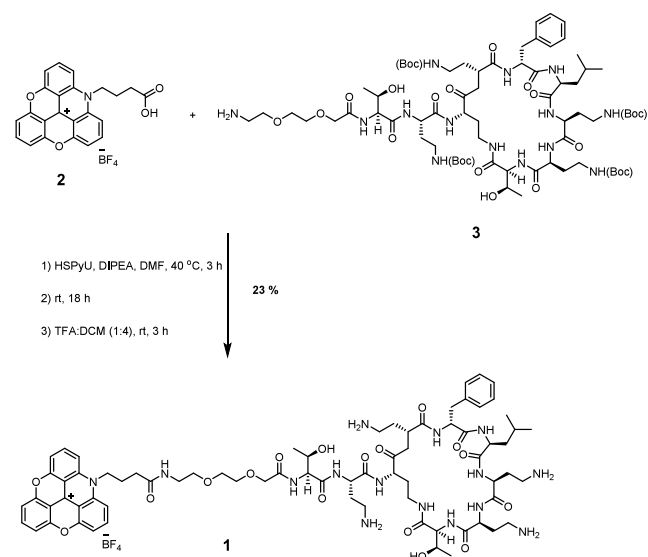
## RESULTS AND DISCUSSION

The synthesis of trioxatriangulenium cations was first reported in 1963 and laid the groundwork for the development of a variety of triangulenium ions that have long fluorescence lifetimes.<sup>34–36</sup> The red-emitting ( $\lambda_{\text{ex}} = 540$  nm and  $\lambda_{\text{em}} = 556$  nm) fluorophore azadioxatriangulenium (ADOTA (2)) can be synthesized with a carboxylic acid group, that can be utilized for coupling to an amine group of a bacteria targeting moiety and was synthesized as reported by Bora et al.<sup>37,38</sup>

The first step in the mechanism of action of PMX is the electrostatic interaction between the positively charged cyclic peptide of PMX and lipid A of bacteria. Therefore, it was important to preserve the structure of PMX when conjugating

the fluorophore to it. Thus, H-(EG)<sub>2</sub>-PMX(Boc)<sub>4</sub> **3**<sup>32</sup> was synthesized (Scheme S8) to leave a single unprotected amine group for amide coupling to the dye. The activating agent HSPyU was used to allow conjugation of ADOTA (2) to compound **3**. The Boc-groups were removed using TFA:DCM to give probe **1** (ADOTA-PMX) (Scheme 1). After

### Scheme 1. Synthesis of the ADOTA-PMX (1) Probe<sup>a</sup>



<sup>a</sup>The carboxylic acid group of the fluorophore **2** was pre-activated using HSPyU and the active ester conjugated to **3**. After the coupling, Boc-deprotection was performed using TFA:DCM (1:4) for 3 h. The final product was obtained after RP-HPLC purification in 23% overall yield.

purification, **1** was characterized using HPLC (Figure S9) and HRMS (Figure S10). Despite the high polarity of the peptide, the probe **1** was poorly soluble in water or saline (due to the flat, planar nature of the dye). Therefore, for biological and photophysical analyses, 1 mM stock solutions were prepared in DMSO and diluted into PBS for application. Probe **1** had a fluorescence quantum yield of 0.68 (Table S11) and identical absorption/emission spectra to ADOTA **2** itself (Figure S1) with absorption and emission bands centered at 540 and 558 nm, respectively.<sup>39</sup>

To determine the selectivity of the synthesized probe, a number of different bacterial strains were incubated with ADOTA-PMX **1** at a range of concentrations (Figure S2). The minimum inhibitory concentration (MIC) of ADOTA-PMX **1** was determined and compared to that of compound **3** (Figure S3). It was found that the MIC of ADOTA-PMX **1** is 2  $\mu\text{M}$ , while compound **3** does not exhibit killing of the bacteria, even at a concentration of 32  $\mu\text{M}$ . Based on this data, imaging was performed using a 1  $\mu\text{M}$  concentration of the probe **1**. As expected, much stronger labeling of *E. coli* (Gram-negative bacteria) was observed, compared to Gram-positive organisms (Figure 1).

Initially, the lifetime of ADOTA-PMX **1** in PBS was measured (560 nm emission) on a spectrofluorometer with a pulsed diode laser ( $\lambda = 451.2$  nm, pulse width = 76.0 ps) as an excitation source and was determined to be  $21.1 \pm 0.1$  ns (mean  $\pm$  S.D.,  $n = 3$ ) (Figure S4), with the long lifetime in agreement with the lifetime values observed for ADOTA derivatives in the literature.<sup>33</sup> The potential of ADOTA-PMX **1**

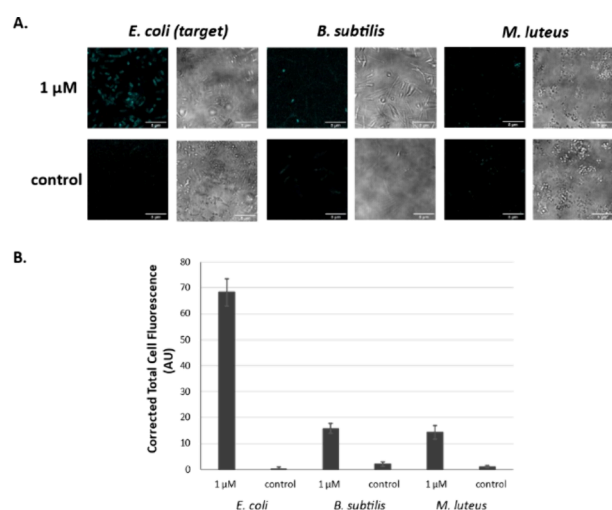


**Figure 1.** Labeling of Gram-negative bacteria with ADOTA-PMX 1. (A) Confocal microscopy images ( $\lambda_{\text{ex}} = 561$  nm) of Gram-negative and Gram-positive bacteria (*E. coli*, *B. subtilis*, *M. luteus*) incubated using the probe 1 (1  $\mu\text{M}$ ) in PBS in darkness at 37 °C for 20 min, before a single wash with PBS prior to imaging. Scale bar = 5  $\mu\text{m}$ . (B) Comparison of the fluorescence intensity of labeled (1  $\mu\text{M}$  ADOTA-PMX) and unlabeled bacteria with target and nontarget bacterial species (calculated using by ImageJ software, Fiji ( $n = 25$ )).

for lifetime imaging applications was subsequently evaluated using a full-spectrum fluorescence lifetime imaging microscope

(FS-FLIM)<sup>24</sup> (for a full description of the system, see the Supporting Information (SI)), using a custom line sensor for single photon counting/detection (Figure 2).<sup>40</sup> This sensor had 512 spectral channels with time-gating for photon arrival from the sample, thus allowing acquisition of fluorescence intensity and lifetime images. *E. coli* stained with ADOTA-PMX 1 were first imaged on the FS-FLIM, with the fluorescence emission spectrum of the bacteria matching that of ADOTA-PMX 1 (Figure 2A), while fluorescence decay curves were generated for each of the 512 wavelengths for each pixel (Figure 2B). Photons arriving at the sensor were time-stamped and segregated into 1.6 ns wide bins, with the number of photons decreasing exponentially over time. These were fit to exponential decay curves to allow the generation of lifetime values (see Figures 2C and S5), and a fluorescence lifetime image across the emission spectrum (500–630 nm) was generated. The characteristic bacterial rodlike shape could be observed in both the intensity (Figure 2D) and lifetime imaging modes (Figure 2E). Interestingly, the probe showed a shorter lifetime when bound to bacteria than in solution (see the histogram of lifetime values for the bacteria in Figure 2C), with most bacteria displaying lifetimes of  $\sim 4.5$  ns. This could be due to the interaction with the bacterial membrane, as well as the quenching mechanisms when the probe conformations are “locked” and the dye molecules were in close proximity. When looking at fields of view that contained clusters of bacteria (denoted by the yellow arrow in Figures S6A and S6B), a second population of brighter, longer lifetime ( $\sim 7$  ns)

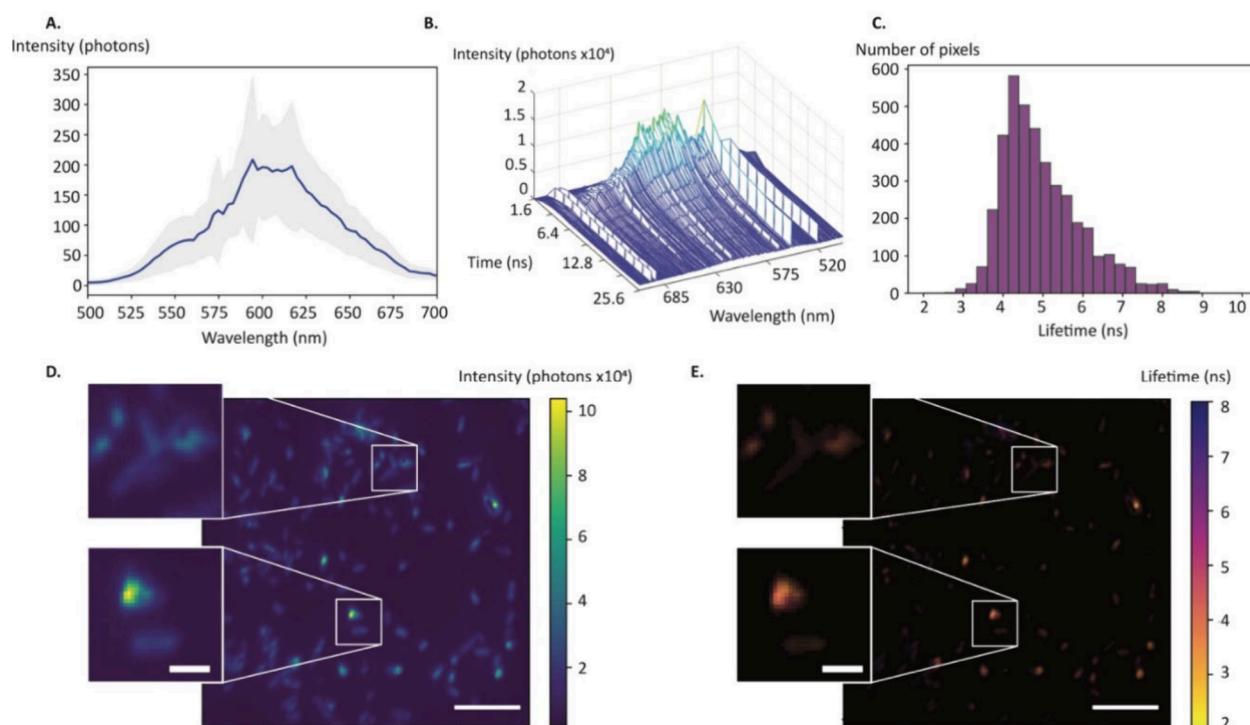


**Figure 2.** Lifetime imaging of *E. coli* stained with lifetime probe ADOTA-PMX 1 (1  $\mu\text{M}$ ) at 37 °C for 20 min. (A) An intensity spectrum of the ADOTA-PMX probe on stained bacteria showed an emission peak at  $\sim 600$  nm. (B) Graph showing how the detector response was recorded for one image pixel. The different wavelengths correspond to singular positions on the 512 SPAD line array. For each of these positions, the incoming photons are time-gated into 1.6 ns wide bins allowing observation/calculation of the fluorescence intensity decays. (C) Histogram of bacterial lifetimes showing the lifetime distribution. (D) Fluorescence intensity image of *E. coli* stained with ADOTA-PMX 1 and imaged on a full spectrum fluorescence lifetime imaging microscope. The intensity was summed across all the detector wavelengths to generate the image. Scale bar = 1  $\mu\text{m}$ . The white boxes represent ROIs that are magnified by a factor of 3, scale bar = 200 nm. (E) Fluorescence lifetime image (false-coloring) showing *E. coli* stained by ADOTA-PMX 1, with zoomed-in panels.

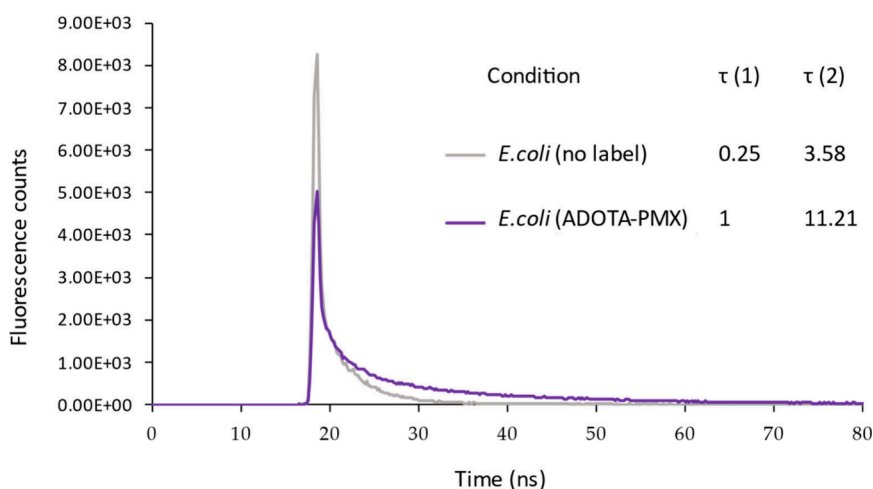


**Figure 3.** Lifetime measurements of ADOTA-PMX labeled Gram-negative bacteria using a spectrofluorometer with a pulsed diode laser ( $\lambda = 451.2$  nm, pulse width 76.0 ps) as an excitation source, and emission set to 560 nm (bandwidth 10 nm). Bacteria were incubated with ADOTA-PMX (1  $\mu$ M) in PBS for 20 min at 37  $^{\circ}$ C, with a single wash with PBS. The measurements were performed in PBS using four clear-sided disposable cuvettes.

bacteria was revealed. The change in the ADOTA-PMX 1 lifetime observed in these could reflect a different metabolic state of activity of the bacteria or extent of probe incorporation into the membrane. In addition, the targeting moiety PMX is an antimicrobial, although here its efficacy was hugely reduced by removal of the lipophilic tail. Nevertheless, the positive charges on PMX can exert an antimicrobial effect on some bacteria; hence, there is a possibility that the lifetime differences relate to clusters of live and dead/inactive bacteria in the field of view. Additionally, we used a benchtop fluorimeter and plastic disposable cuvettes to measure lifetime of the ADOTA-PMX-labeled bacteria. This showed that labeled bacteria had much longer lifetimes (11.2 ns), compared to unlabeled bacteria that showed autofluorescence lifetimes of 3.6 ns (Figure 3). This demonstrates that bacteria detection can be performed within minutes without the need for a sophisticated microscope. Using the same protocol, the lifetime of ADOTA-PMX labeling was compared between *E. coli* and *B. subtilis* (Figure S7). Similar lifetimes (11 ns) were observed for *B. subtilis*, although with much weaker photon counts for the same number of bacteria (by optical density), relating to the presence of some interaction between bacteria and the probe aligning with the results of the selectivity test using fluorescent microscopy (see Figure 1).

## CONCLUSIONS

In conclusion, ADOTA-PMX 1 is the first example of a targeted probe for bacterial fluorescence lifetime imaging. This probe showed good selectivity and sensitivity emphasizing its applicability in screening of Gram-negative bacteria. Long fluorescence lifetime allows the probe being distinguished from other fluorophores and autofluorescence, enabling multiplexing, or simultaneous imaging of multiple molecular species. The sensitivity of fluorescence lifetime advantages and simplifies bacteria detection protocols with the use of simple benchtop instruments. Future work may focus on improving probe solubility, enhancing selectivity, and exploring the full range of its applications in clinical and environmental microbiology.

## ASSOCIATED CONTENT

### Supporting Information

The Supporting Information is available free of charge at <https://pubs.acs.org/doi/10.1021/cbmi.4c00066>.

HPLC and HRMS data for ADOTA-PMX, photo-physical characterizations of ADOTA-PMX, MIC assay, confocal microscopy imaging, fluorescence lifetime imaging, general information, and experimental procedures (PDF)

## AUTHOR INFORMATION

### Corresponding Author

Mark Bradley – Precision Healthcare University Research Institute, Queen Mary University of London, Whitechapel, London E1 4NS, United Kingdom; [orcid.org/0000-0001-7893-1575](https://orcid.org/0000-0001-7893-1575); Email: [m.bradley@qmul.ac.uk](mailto:m.bradley@qmul.ac.uk)

### Authors

Assel Baibek – School of Chemistry, University of Edinburgh, Edinburgh EH9 3FJ, United Kingdom; [orcid.org/0009-0000-0027-3883](https://orcid.org/0009-0000-0027-3883)

Zuzanna Konieczna – School of Chemistry, University of Edinburgh, Edinburgh EH9 3FJ, United Kingdom; Chemistry Hub, Institute for Regeneration and Repair, University of Edinburgh, Edinburgh EH16 4UU, United Kingdom

Muhammed Üçüncü – Department of Analytical Chemistry, Faculty of Pharmacy, İzmir Katip Çelebi University, 35620 İzmir, Turkey; [orcid.org/0000-0001-6200-9340](https://orcid.org/0000-0001-6200-9340)

Zainab S. Alghamdi – Department of Chemistry, College of Science, Imam Abdulrahman Bin Faisal University, Dammam 31441, Saudi Arabia; [orcid.org/0009-0006-8926-162X](https://orcid.org/0009-0006-8926-162X)

Richa Sharma – School of Chemistry, University of Edinburgh, Edinburgh EH9 3FJ, United Kingdom; [orcid.org/0000-0003-1567-1176](https://orcid.org/0000-0003-1567-1176)

Mathew H. Horrocks – School of Chemistry, University of Edinburgh, Edinburgh EH9 3FJ, United Kingdom; Chemistry Hub, Institute for Regeneration and Repair, University of Edinburgh, Edinburgh EH16 4UU, United Kingdom; [orcid.org/0000-0001-5495-5492](https://orcid.org/0000-0001-5495-5492)

Complete contact information is available at:

<https://pubs.acs.org/10.1021/cbmi.4c00066>

### Author Contributions

The manuscript was written through contributions of all authors. All authors have given approval to the final version of the manuscript.

### Funding

This research was funded by Engineering and Physical Sciences Research Council (EPSRC, United Kingdom) Interdisciplinary Research Collaboration, Grant Nos. EP/K03197X/1 and EP/R005257/1. The FS-FLIM microscope was funded by a Royal Society, Grant No. RGS\R1\201163. Z.K. is funded via the BBSRC EastBIO doctoral training program, grant BB/M010996/1. R.S. was funded by a Newton-Bhabha International Fellowship from The Royal Society, UK and The Science and Engineering Research Board, India, Grant No. NIF/R1/192688.

### Notes

The authors declare no competing financial interest.

### ACKNOWLEDGMENTS

We acknowledge Hazel Stewart and Gareth Williams for their help in building the FS-FLIM used for the measurements, Gavin Birch for initial work in synthesis and Annamaria Lilienkampf for supervision.

### REFERENCES

- (1) World Health Organisation. Global action plan on antimicrobial resistance, 2015.
- (2) World Health Organisation. Antimicrobial resistance: global report on surveillance, 2014.
- (3) Marshall, A. P.; Shirley, J. D.; Carlson, E. E. Enzyme-targeted fluorescent small-molecule probes for bacterial imaging. *Curr. Opin. Chem. Biol.* **2020**, *57*, 155–165.
- (4) Cambré, A.; Aertsen, A., Bacterial Vivisection: How Fluorescence-Based Imaging Techniques Shed a Light on the Inner Workings of Bacteria. *Microbiol. Mol. Biol. Rev.* **2020**, *84* (4), DOI: [DOI: 10.1128/MMBR.00008-20](https://doi.org/10.1128/MMBR.00008-20).
- (5) Stone, M. R. L.; Butler, M. S.; Phetsang, W.; Cooper, M. A.; Blaskovich, M. A. T. Fluorescent Antibiotics: New Research Tools to Fight Antibiotic Resistance. *Trends Biotechnol.* **2018**, *36* (5), 523–536.
- (6) Zhao, G.; Meier, T. I.; Kahl, S. D.; Gee, K. R.; Blaszcak, L. C. BOCILLIN FL, a sensitive and commercially available reagent for detection of penicillin-binding proteins. *Antimicrob. Agents Chemother.* **1999**, *43* (5), 1124–1128.
- (7) Kocaoglu, O.; Calvo, R. A.; Sham, L. T.; Cozy, L. M.; Lanning, B. R.; Francis, S.; Winkler, M. E.; Kearns, D. B.; Carlson, E. E. Selective penicillin-binding protein imaging probes reveal substructure in bacterial cell division. *ACS Chem. Biol.* **2012**, *7* (10), 1746–1753.
- (8) Zlokarnik, G.; Negulescu, P. A.; Knapp, T. E.; Mere, L.; Bures, N.; Feng, L. X.; Whitney, M.; Roemer, K.; Tsien, R. Y. Quantitation of transcription and clonal selection of single living cells with  $\beta$ -lactamase as reporter. *Science* **1998**, *279* (5347), 84–88.
- (9) Akhtar, M. S.; Qaisar, A.; Irfanullah, J.; Iqbal, J.; Khan, B.; Jehangir, M.; Nadeem, M. A.; Khan, M. A.; Afzal, M. S.; Ul-Haq, I.; Imran, M. B. Antimicrobial peptide 99mTc-ubiquicidin 29–41 as human infection-imaging agent: Clinical trial. *J. Nucl. Med.* **2005**, *46* (4), 567–573.
- (10) Akram, A. R.; Avlonitis, N.; Lilienkampf, A.; Perez-Lopez, A. M.; McDonald, N.; Chankeshwara, S. V.; Scholefield, E.; Haslett, C.; Bradley, M.; Dhaliwal, K. A labelled-ubiquicidin antimicrobial peptide for immediate in situ optical detection of live bacteria in human alveolar lung tissue. *Chem. Sci.* **2015**, *6* (12), 6971–6979.
- (11) Akram, A. R.; Avlonitis, N.; Scholefield, E.; Vendrell, M.; McDonald, N.; Aslam, T.; Craven, T. H.; Gray, C.; Collie, D. S.; Fisher, A. J.; Corris, P. A.; Walsh, T.; Haslett, C.; Bradley, M.; Dhaliwal, K. Enhanced avidity from a multivalent fluorescent antimicrobial peptide enables pathogen detection in a human lung model. *Sci. Rep.* **2019**, *9* (1), 8422.
- (12) Chen, H.; Liu, C.; Chen, D.; Madrid, K.; Peng, S.; Dong, X.; Zhang, M.; Gu, Y. Bacteria-Targeting Conjugates Based on Antimicrobial Peptide for Bacteria Diagnosis and Therapy. *Mol. Pharmaceutics* **2015**, *12* (7), 2505–2516.
- (13) Welling, M. M.; de Korne, C. M.; Spa, S. J.; van Willigen, D. M.; Hensbergen, A. W.; Bunschoten, A.; Duszenko, N.; Smits, W. K.; Roestenberg, M.; van Leeuwen, F. W. B. Multimodal Tracking of Controlled Staphylococcus aureus Infections in Mice. *ACS Infect. Dis.* **2019**, *5* (7), 1160–1168.
- (14) Butler, M. S.; Hansford, K. A.; Blaskovich, M. A.; Halai, R.; Cooper, M. A. Glycopeptide antibiotics: back to the future. *J. Antibiot. (Tokyo)* **2014**, *67* (9), 631–644.
- (15) Hildebrandt, P.; Surmann, K.; Salazar, M. G.; Normann, N.; Volker, U.; Schmidt, F. Alternative fluorescent labeling strategies for characterizing gram-positive pathogenic bacteria: Flow cytometry supported counting, sorting, and proteome analysis of Staphylococcus aureus retrieved from infected host cells. *Cytometry A* **2016**, *89* (10), 932–940.
- (16) Wang, W.; Zhu, Y.; Chen, X. Selective Imaging of Gram-Negative and Gram-Positive Microbiotas in the Mouse Gut. *Biochemistry* **2017**, *56* (30), 3889–3893.
- (17) van Oosten, M.; Schäfer, T.; Gazendam, J. A. C.; Ohlsen, K.; Tsompanidou, E.; de Goffau, M. C.; Harmsen, H. J. M.; Crane, L. M. A.; Lim, E.; Francis, K. P.; Cheung, L.; Olive, M.; Ntziachristos, V.; van Dijl, J. M.; van Dam, G. M. Real-time in vivo imaging of invasive and biomaterial-associated bacterial infections using fluorescently labelled vancomycin. *Nat. Commun.* **2013**, *4* (1), 2584.
- (18) Mills, B.; Megia-Fernandez, A.; Norberg, D.; Duncan, S.; Marshall, A.; Akram, A. R.; Quinn, T.; Young, I.; Bruce, A. M.; Scholefield, E.; Williams, G. O. S.; Krstajić, N.; Choudhary, T. R.; Parker, H. E.; Tanner, M. G.; Harrington, K.; Wood, H. A. C.; Birks, T. A.; Knight, J. C.; Haslett, C.; Dhaliwal, K.; Bradley, M.; Uccuncu, M.; Stone, J. M. Molecular detection of Gram-positive bacteria in the human lung through an optical fiber-based endoscope. *Eur. J. Nucl. Med.* **2021**, *48* (3), 800–807.
- (19) Sharma, R.; Rajagopalan, H.; Klausen, M.; Jeyalatha, M. V.; Üçüncü, M.; Venkateswaran, S.; Anand, A. R.; Bradley, M. Rapid detection of major Gram-positive pathogens in ocular specimens using a novel fluorescent vancomycin-based probe. *Sens. Diagn.* **2022**, *1* (5), 1014–1020.
- (20) Phetsang, W.; Blaskovich, M. A. T.; Butler, M. S.; Huang, J. X.; Zuegg, J.; Mamidyala, S. K.; Ramu, S.; Kavanagh, A. M.; Cooper, M. A. An azido-oxazolidinone antibiotic for live bacterial cell imaging and generation of antibiotic variants. *Bioorg. Med. Chem.* **2014**, *22* (16), 4490–4498.
- (21) Datta, R.; Heaster, T. M.; Sharick, J. T.; Gillette, A. A.; Skala, M. C. Fluorescence lifetime imaging microscopy: fundamentals and advances in instrumentation, analysis, and applications. *J. Biomed. Opt.* **2020**, *25* (7), 1–43.
- (22) Magde, D.; Rojas, G. E.; Seybold, P. G. Solvent Dependence of the Fluorescence Lifetimes of Xanthene Dyes. *Photochem. Photobiol.* **1999**, *70* (5), 737–744.
- (23) Hanson, K. M.; Behne, M. J.; Barry, N. P.; Mauro, T. M.; Gratton, E.; Clegg, R. M. Two-photon fluorescence lifetime imaging of the skin stratum corneum pH gradient. *Biophys. J.* **2002**, *83* (3), 1682–1690.
- (24) Williams, G. O. S.; Williams, E.; Finlayson, N.; Erdogan, A. T.; Wang, Q.; Fernandes, S.; Akram, A. R.; Dhaliwal, K.; Henderson, R. K.; Girkin, J. M.; Bradley, M. Full spectrum fluorescence lifetime imaging with 0.5 nm spectral and 50 ps temporal resolution. *Nat. Commun.* **2021**, *12* (1), 6616.
- (25) Kang, J.; Lhee, S.; Lee, J. K.; Zare, R. N.; Nam, H. G. Restricted intramolecular rotation of fluorescent molecular rotors at the

periphery of aqueous microdroplets in oil. *Sci. Rep.* **2020**, *10* (1), No. 16859.

(26) Lin, S.; Struve, W. S. Time-resolved fluorescence of nitrobenzoxadiazole-aminohexanoic acid: effect of intermolecular hydrogen-bonding on non-radiative decay. *Photochem. Photobiol.* **1991**, *54* (3), 361–365.

(27) Luan, J.; Seth, A.; Gupta, R.; Wang, Z.; Rathi, P.; Cao, S.; Gholami Derami, H.; Tang, R.; Xu, B.; Achilefu, S.; Morrissey, J. J.; Singamaneni, S. Ultrabright fluorescent nanoscale labels for the femtomolar detection of analytes with standard bioassays. *Nat. Biomed. Eng.* **2020**, *4* (5), 518–530.

(28) Berezin, M. Y.; Achilefu, S. Fluorescence lifetime measurements and biological imaging. *Chem. Rev.* **2010**, *110* (5), 2641–2684.

(29) Wang, W.; Chen, X. Antibiotics-based fluorescent probes for selective labeling of Gram-negative and Gram-positive bacteria in living microbiotas. *Sci. China Chem.* **2018**, *61* (7), 792–796.

(30) Akram, A. R.; Chankeshwara, S. V.; Scholefield, E.; Aslam, T.; McDonald, N.; Megia-Fernandez, A.; Marshall, A.; Mills, B.; Avlonitis, N.; Craven, T. H.; Smyth, A. M.; Collie, D. S.; Gray, C.; Hirani, N.; Hill, A. T.; Govan, J. R.; Walsh, T.; Haslett, C.; Bradley, M.; Dhaliwal, K., In situ identification of Gram-negative bacteria in human lungs using a topical fluorescent peptide targeting lipid A. *Sci. Transl. Med.* **2018**, *10* (464). DOI: [DOI: 10.1126/scitranslmed.aal0033](https://doi.org/10.1126/scitranslmed.aal0033).

(31) Megia-Fernandez, A.; Klausen, M.; Mills, B.; Brown, G. E.; McEwan, H.; Finlayson, N.; Dhaliwal, K.; Bradley, M. Red-Shifted Environmental Fluorophores and Their Use for the Detection of Gram-Negative Bacteria. *Chemosensors* **2021**, *9* (6), 117.

(32) Ucuncu, M.; Mills, B.; Duncan, S.; Staderini, M.; Dhaliwal, K.; Bradley, M. Polymyxin-based photosensitizer for the potent and selective killing of Gram-negative bacteria. *Chem. Commun.* **2020**, *56* (26), 3757–3760.

(33) Bogh, S. A.; Bora, I.; Rosenberg, M.; Thyraug, E.; Laursen, B. W.; Sørensen, T. J. Azadioxatriangulenium: exploring the effect of a 20 ns fluorescence lifetime in fluorescence anisotropy measurements. *Methods Appl. Fluoresc.* **2015**, *3* (4), No. 045001.

(34) Laursen, B. W.; Krebs, F. C. Synthesis, Structure, and Properties of Azatriangulenium Salts. *Chem.—Eur. J.* **2001**, *7* (8), 1773–1783.

(35) Sørensen, T. J.; Laursen, B. W. Synthesis and Optical Properties of Trioxatriangulenium Dyes with One and Two Peripheral Amino Substituents. *J. Org. Chem.* **2010**, *75* (18), 6182–6190.

(36) Laursen, B. W.; Sørensen, T. J. Synthesis of Super Stable Triangulenium Dye. *J. Org. Chem.* **2009**, *74* (8), 3183–3185.

(37) Bora, I.; Bogh, S. A.; Rosenberg, M.; Santella, M.; Sørensen, T. J.; Laursen, B. W. Diazoatriangulenium: synthesis of reactive derivatives and conjugation to bovine serum albumin. *Org. Biomol. Chem.* **2016**, *14* (3), 1091–1101.

(38) Bora, I.; Bogh, S. A.; Santella, M.; Rosenberg, M.; Sørensen, T. J.; Laursen, B. W. Azadioxatriangulenium: Synthesis and Photo-physical Properties of Reactive Dyes for Bioconjugation. *Eur. J. Org. Chem.* **2015**, *2015* (28), 6351–6358.

(39) Maliwal, B. P.; Fudala, R.; Raut, S.; Kokate, R.; Sørensen, T. J.; Laursen, B. W.; Gryczynski, Z.; Gryczynski, I. Long-lived bright red emitting azaoxa-triangulenium fluorophores. *PLoS One* **2013**, *8* (5), No. e63043.

(40) Erdogan, A. T.; Walker, R.; Finlayson, N.; Krstajić, N.; Williams, G.; Girkin, J.; Henderson, R. A CMOS SPAD Line Sensor With Per-Pixel Histogramming TDC for Time-Resolved Multispectral Imaging. *IEEE J. Solid-State Circuits* **2019**, *54* (6), 1705–1719.